Photogrammetry for Non-Invasive Terrestrial Position/Velocity Measurement of High-Flying Aircraft

Part I

James A Crawford

Synopsis

I have had an interest in astronomy since high school days. More precisely, I have had an interest in astronomical instruments and the associated calculation of position and velocity since that time. This project is intended to be the first step in a progression of projects which build upon each other, culminating in a fully remote-controlled astronomical observatory.

In this project, two remote-controlled telescopes equipped with CCD cameras will be positioned roughly 1,000 feet apart and actively trained on high flying jets overhead to ascertain vectorial position and velocity (PV) solutions using triangulation combined with mathematical techniques. The tie-in with astronomy is that (i) equatorial telescope mounts will be used and (ii) the night-time star field will be used to precisely align the two telescopes so that precise triangulation can be performed down to the CCD pixel level. From the mathematical perspective, Kalman filter techniques will be used to refine the raw optical measurements. Kalman filter techniques will also be used in a subsequent project where LEO/MEO satellites will be the objects of interest.

1 Getting Started

My local geography is situated within clear site of several flight paths from airports in the southern California area. As such, there is usually a jet overhead and in view every few minutes. One random photo of a plane overhead is shown in Figure 1 and Figure 2. The photo shown in Figure 2 invites a lot of “what if” speculation about what types of information could be extracted from the instrumentation. For instance:

- Airplane position and velocity of course, in vectorial form
- Translate PV details to different display formats like Google Maps, including altitude
- Even with only a 200 mm lens, pixel-level image tracking can track different plane features, like engines, nose, tail, wings
- Plane model details (e.g., Airbus , Boeing 737)
- Catalog how closely different flights follow the same path in the sky
- Assess atmosphere transparency versus look angle
- Measure atmosphere-related refraction
- Use the raw data extracted to improve mathematical modeling techniques (e.g., Kalman filtering)

Figure 1 70mm full-frame picture of one plane overhead

Figure 2 Same flight using 200mm f/2.8 lens with high digital zoom (Canon 5D)

This project will require efforts in multiple areas including at a minimum:

- Telescope optics
- CCD camera details and proper attachment to the telescope
- Telescope mount and associated precision servo drives
- Wireless telemetry and control of the telescope mount
- Wireless control of the CCD camera and retrieval of digital images
- Battery with solar-charging to alleviate any cabling
- GUI and user software on a PC laptop
- Image *stacking* and scintillation removal using image processing
- Image analysis
- Star field calibration software for initial telescope alignment
- Image-based tracking with trajectory prediction (Kalman filter based)

I already have a working telemetry link via WiFi up and operational using an Arduino Mega2560. The link connects to my home's WiFi network and I can communicate to and from the Mega via a GUI interface written in C# which will run on any networked PC I wish. I also have one of two required equatorial telescope mounts (see Figure 3) and one suitable telescope (see Figure 4). I also have two solar panels and rechargeable batteries for the power sources. My CNC machine will most likely help in fabrication of needed mounting hardware to help keep costs down.

In astronomical work, particularly deep-sky photography, the quality of the telescope mount is by far the most important ingredient of everything listed above. The old rule of thumb used to be that you should spend 2/3 of your budget on the mount, leaving 1/3 for the telescope. For serious deep-sky work, that ratio may have actually moved up to ¾. Telescope mount integrity for this project will not be nearly as demanding, but pointing repeatability is a necessary performance metric which must be closely watched.

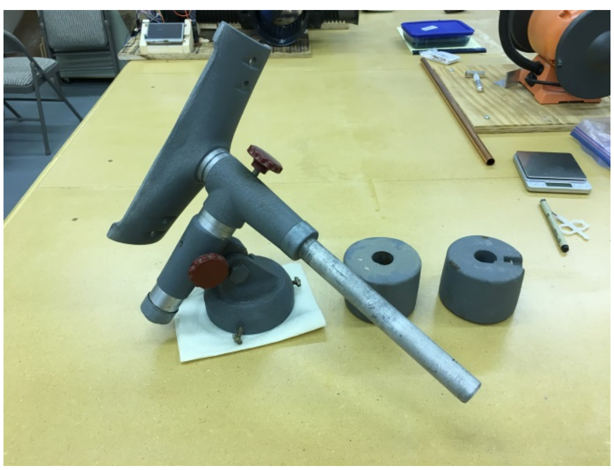

Figure 3 One of the two equatorial telescope mounts required

Figure 4 One of the two telescopes required

2 Telescope Angular Resolution Requirements

In order to get an idea about the angular resolution involved, consider the idealized situation shown in Figure 5. Since the airplane's altitude h is very small compared to the radius of the earth R_e, the maximum slant-range r to the aircraft is closely given by[1]

$$r_{\max} = \sqrt{2R_e h} \tag{1}$$

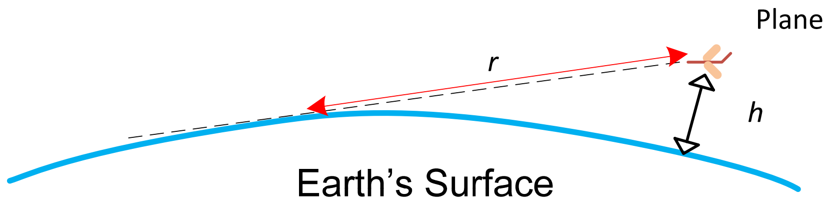

Figure 5 Slant range (r) to distant aircraft flying at altitude h above spherical earth

The slant-range r is computed for several different altitudes and elevation angles[2] in Table 1. The four right-hand columns show the angle extended by a 10 foot feature on the plane in terms of seconds of a degree. To put this into some context, the theoretical resolution limit of a circular telescope aperture (in free space) is approximately given by

$$ResolvingPower_{seconds} \cong \frac{5}{D_{inches}} \tag{2}$$

where D_{inches} is the diameter of the telescope's objective lens in inches. Since a 2" lens diameter (e.g., 50 mm binoculars) is sufficient to theoretically resolve about 2.5 seconds of arc, resolving 18 seconds (finest resolution in Table 1) should not present a problem for a reasonable optical telescope. Atmospheric turbulence will present more of an issue.

From a practical standpoint, no more optical magnification should be used than necessary in order to make getting the airplane initially into view easier. To this end, the telescope optics should also be reasonably well matched with the CCD pixel size of the camera being used.

Table 1 Slant Range as a Function of Airplane Height h and Elevation Angle[3] (Feature Size = 10 ft)

	Max to Horizon			Max Slant-Range with Elevation Angle, deg					Feature Size in Seconds of Angle			
h, feet	r max, feet	rmax, miles		89	70	50	20		89	70	50	20
3,000	355,977.5	67.42		3,000	3,193	3,916	8,767		687	646	527	235
5,000	459,565.0	87.04		5,001	5,321	6,526	14,606		412	388	316	141
10,000	649,923.1	123.09		10,002	10,641	13,052	29,186		206	194	158	71
15,000	795,989.9	150.76		15,002	15,962	19,576	43,740		137	129	105	47
20,000	919,130.0	174.08		20,003	21,282	26,099	58,269		103	97	79	35
25,000	1,027,618.6	194.62		25,004	26,602	32,622	72,772		82	78	63	28
30,000	1,125,699.8	213.20		30,005	31,922	39,143	87,250		69	65	53	24
35,000	1,215,894.7	230.28		35,005	37,242	45,663	101,702		59	55	45	20
40,000	1,299,846.1	246.18		40,006	42,562	52,182	116,129		52	48	40	18

[1] From Pythagorean theorem, $r = \sqrt{\left(R_e + h\right)^2 - R_e^2} = \sqrt{2R_e h + h^2} \cong \sqrt{2R_e h}$

[2] Elevation angle is measured relative to the horizon.

[3] From U24868.

2.1 Matching Telescope Optics to CCD/CMOS Camera Sensor

Two approximations can be used to compute how well a candidate telescope and CCD sensor are matched. The total field of view for a given telescope main objective is given by[4]

$$FoV_{\text{arc-minutes}} = \frac{3438 L_{ccd-mm}}{L_{obj-mm}} \tag{3}$$

where

L_{ccd-mm}	CCD dimension of interest in mm
L_{obj-mm}	Focal length of the telescope's objective in mm

The *FoV* calculation is an important factor for initially capturing the airplane in view. As a point of reference, the moon extends an angle of about 0.5 degrees of arc.

The second approximation is for the resolving power per CCD pixel given by

$$R_{pixel-arc\sec} = \frac{206265 \times L_{pixel-\dim-mm}}{L_{obj-mm}} \tag{4}$$

where

$L_{pixel-\dim-mm}$	Pixel dimension of interest in mm
L_{obj-mm}	Focal length of the telescope's objective in mm

Information for several different CCD sensors is provided in Table 2. The last two table entries are from inexpensive camera listings on Amazon. Equations (3) and (4) are plotted for these sensors in Figure 6 through Figure 8. Of the CCD sensors considered, the Arducam 5-MP is the hands-down winner because it is far cheaper than a Canon 5D and its resolution and field of view are outstanding even with a 20-inch telescope objective. If this camera were to be used with the telescope shown in Figure 4, a focal-reducer would likely be desirable. It may actually be better to purchase a new telescope with an objective focal length on the order of 15 inches since this would represent less weight, and wind-loading much less since the cross-sectional area of the smaller scope would be considerably less.

Table 2 CCD Sensor Examples

CCD Sensor	Dimensions (mm)	Mega-Pixels	Pixel Size, μm
Canon 5D	36 x 24	23.4	6.25
Videoorg Mini FPV Voltage 1000TVL	8.5 x 8.5	768 x 576	12.8
Arducam-Mini-5MP-Plus	34 x 24	5	1.4 x 1.4

[4] From U15516, *My Notes*, Vol. 14.

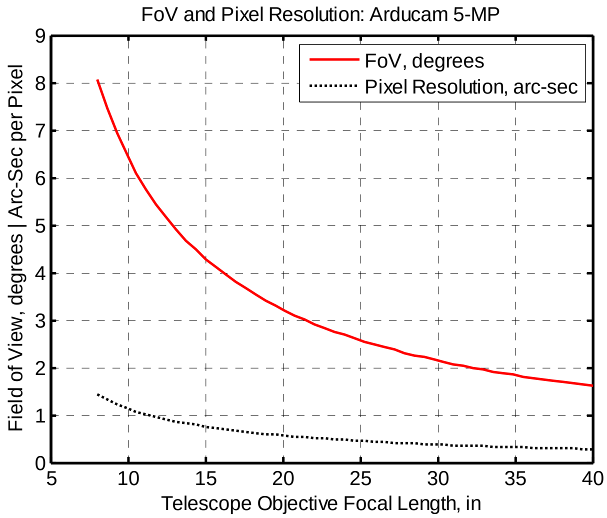

Figure 6 FoV and pixel resolution for the Arducam 5-MP sensor[5]

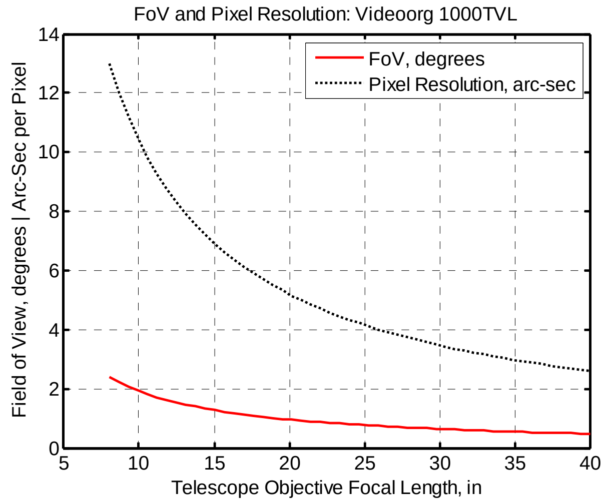

Figure 7 FoV and pixel resolution for the Videoorg 1000TVL

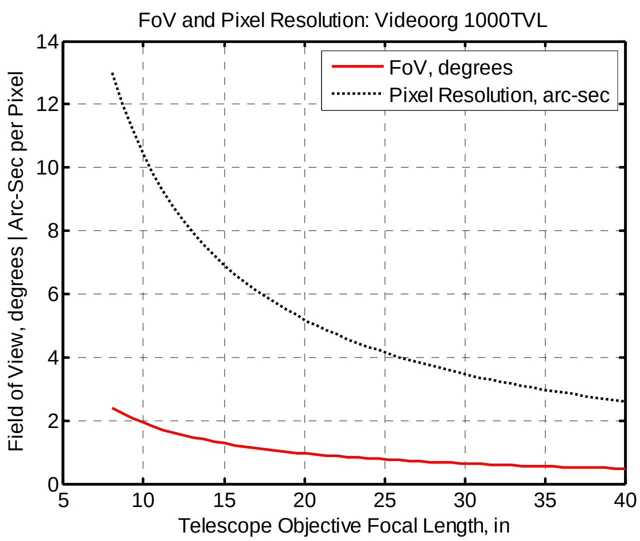

Figure 8 FoV and pixel resolution for the Canon 5D

2.2 Angular Slew Rate for Tracking

Astronomical telescope mounts are not built for speed. If a standard telescope mount is used, it is wise to ensure that it has sufficient speed for the job. The worst-case angular slew rate will occur when the plane is directly overhead. Assuming a minimum plane altitude of 10,000 feet and velocity of 650 miles per hour to be conservative, the maximum angular slew rate will be about 5.5^{o} per second. The larger the telescope (i.e., weight), the more difficult this high slew rate will be to deliver accurately.

5 From U24869_camera_scope_match.m.

2.3 Triangulation Mathematics

Ground-distance between the observation points and the airplane's projection on to the earth may easily reach 20 miles depending upon the airplane's altitude. The change in height due to the earth's curvature over that distance is closely given by

$$\Delta h = \frac{d^2}{2R_e} \tag{5}$$

leading to $\Delta h \approx 265 \text{ ft}$ over that distance. Consequently, earth curvature needs to be included in the calculation if good accuracy is to be achieved. Nevertheless, the following discussion assumes a flat earth for the time being.

2.3.1 Flat Earth

The observational coordinate system for this discussion is shown in Figure 9 where it is assumed without any real loss of generality that $(x_1, y_1, z_1) = (0,0,0)$. All distances will be assumed to be feet unless otherwise specified. Astronomical coordinates are usually specified in terms of right-ascension and declination, but rectangular coordinates are used here for greater simplicity.

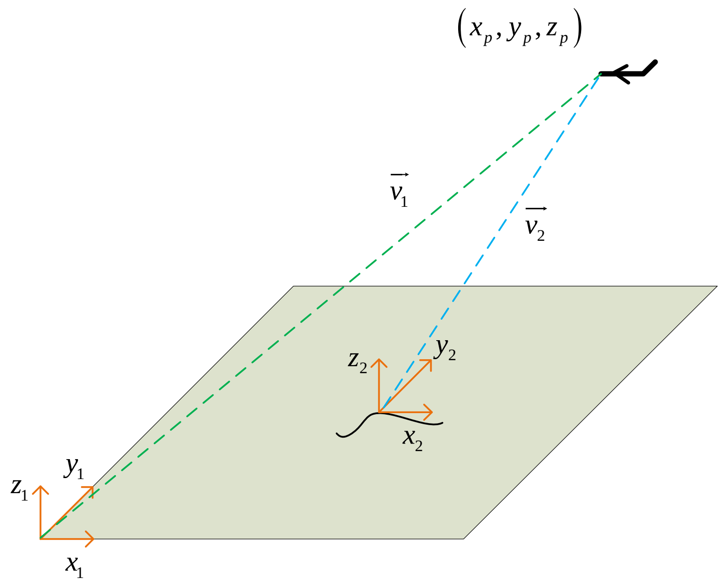

Figure 9 Flat earth observation of an overhead aircraft

Line of sight vectors $\vec{v_1}$ and $\vec{v_2}$ are given by

$$\vec{v_1} = x_p \hat{i} + y_p \hat{j} + z_p \hat{k} \tag{6}$$

$$\vec{v_1} = (x_p - x_2)\hat{i} + (y_p - y_2)\hat{j} + (z_p - z_2)\hat{k} \tag{7}$$

with $\hat{i}, \hat{j}, \text{and } \hat{k}$ the usual unit vectors in the direction of the x, y, and z directions. The direction cosines are easily computed as

$$k_1 = \cos\left(\theta_{az1}\right) = \frac{x_p}{\sqrt{x_p^2 + y_p^2 + z_p^2}}$$
$$k_2 = \cos\left(\theta_{el1}\right) = \frac{z_p}{\sqrt{x_p^2 + y_p^2 + z_p^2}} \quad (8)$$

and

$$k_3 = \cos\left(\theta_{az2}\right) = \frac{x_p - x_2}{\sqrt{\left(x_p - x_2\right)^2 + \left(y_p - y_2\right)^2 + \left(z_p - z_2\right)^2}}$$
$$k_4 = \cos\left(\theta_{el2}\right) = \frac{z_p - z_2}{\sqrt{\left(x_p - x_2\right)^2 + \left(y_p - y_2\right)^2 + \left(z_p - z_2\right)^2}} \quad (9)$$

From (8), it easily follows that

$$\frac{x_p}{z_p} = \frac{k_1}{k_2} \quad (10)$$

and from (9) that

$$\frac{k_3}{k_4} = \frac{x_p - x_2}{z_p - z_2} \quad (11)$$

From these last two equations and a small amount of algebra, the *z*-coordinate of the airplane is given by

$$z_p = \frac{k_2 k_4 \left(x_2 - \frac{k_3}{k_4} z_2 \right)}{k_1 k_4 - k_2 k_3} \quad (12)$$

Calculation of the airplane's altitude turns out to be much more sensitive to measurement errors than estimating azimuth and elevation angles. This *dilution of precision* for altitude is a common problem associated with look-angles from the observation points to the aircraft. The same kind of dilution is a serious topic for GPS location determination as well.

It is helpful to have some idea about angular precision needs before committing to a serious hardware/software development effort. Since altitude determination is the most sensitive to precision, measurement errors in the two pairs of azimuth and elevation angles were assumed and (12) subsequently used to compute the resultant altitude. For now, the angular measurement errors were assumed to follow an unbiased Gaussian distribution. In the example results that follow, it is assumed that $\left(x_2, y_2, z_2\right) = \left(600, 0, 20\right)$.

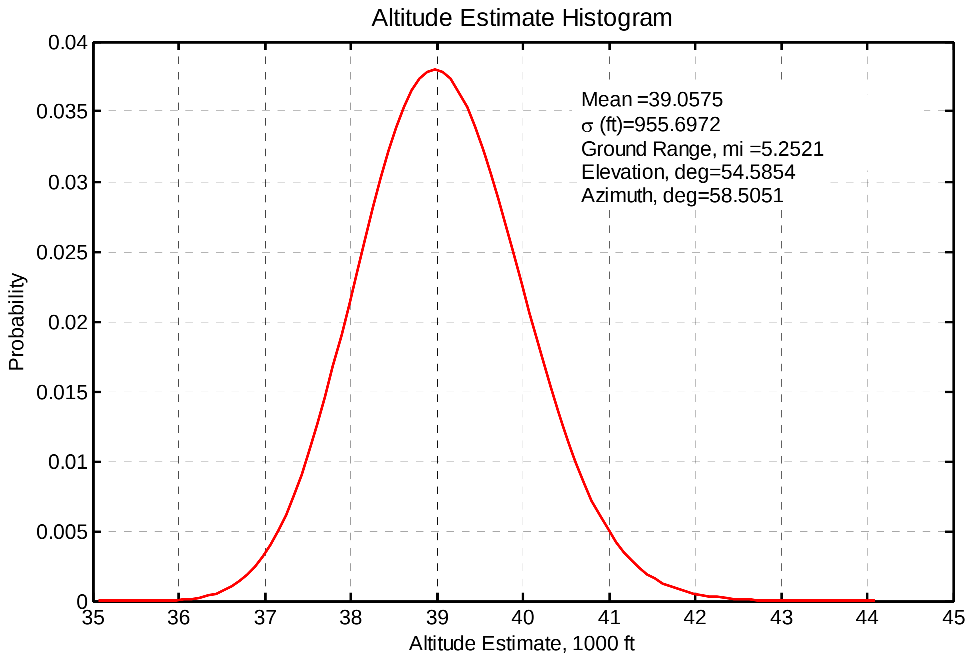

Figure 10 $\left(x_p, y_p, z_p\right) = \left(25000, 12000, 39000\right)$ with the standard deviation for all of the direction cosine angles being 50 seconds of arc

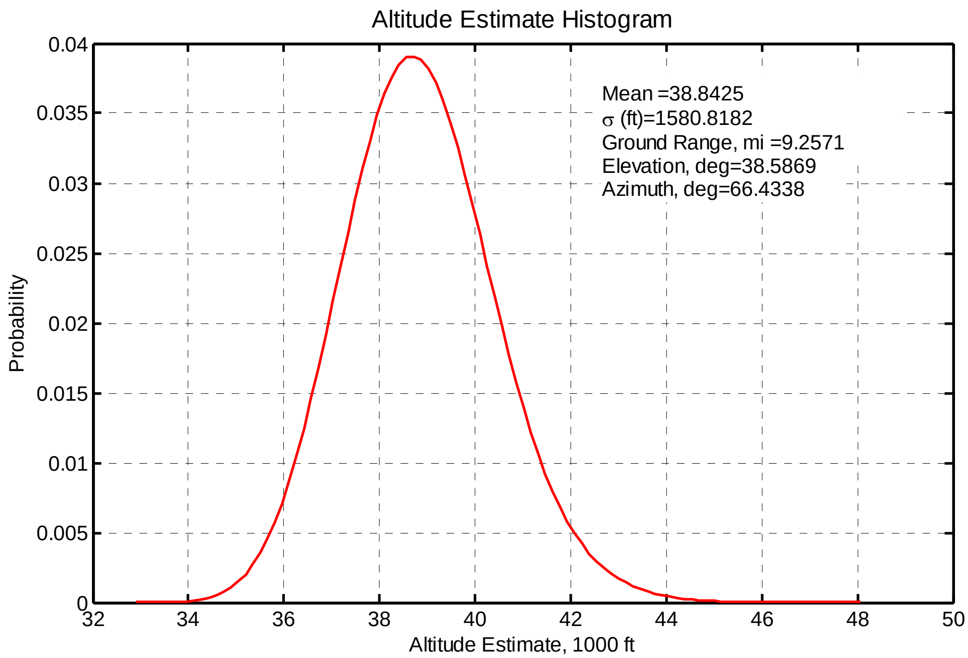

Figure 11 $\left(x_p, y_p, z_p\right) = \left(25000, 42000, 39000\right)$ with the standard deviation for all of the direction cosine angles being 50 seconds of arc. Even though the plane's elevation angle is reasonable, note that the standard deviation for the altitude estimate is nearly 1,600 feet.

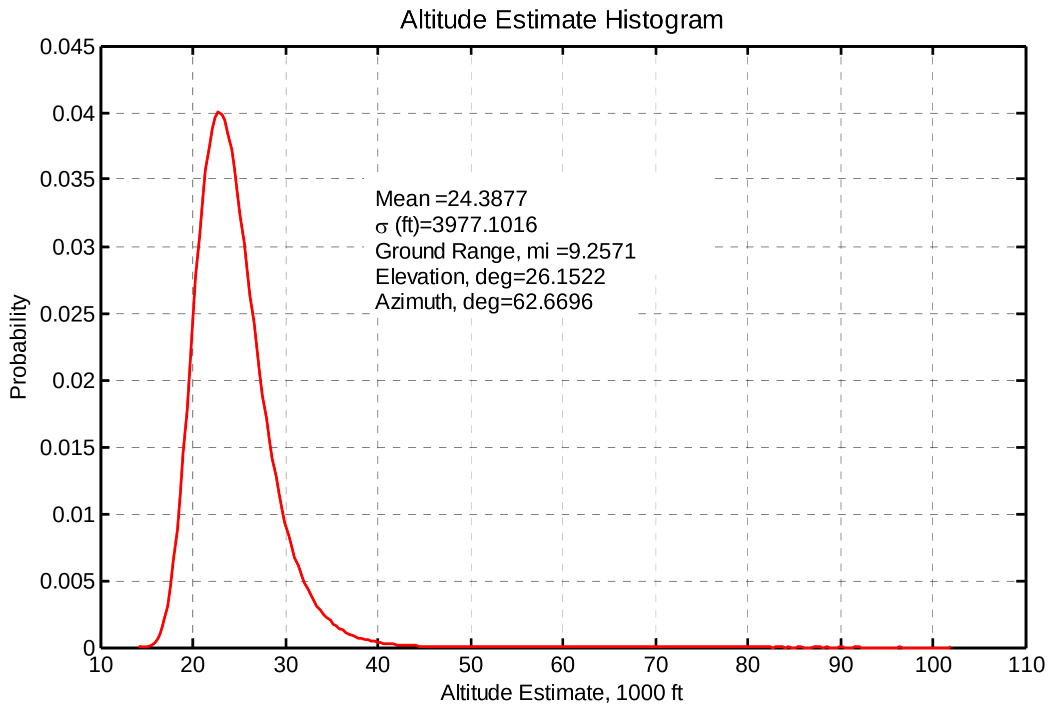

Figure 12 $(x_p, y_p, z_p) = (25000, 42000, 24000)$ with the standard deviation for all of the direction cosine angles being 180 seconds (same as 3 minutes) of arc. Note that the standard deviation of the plane's altitude is quite poor at almost 4,000 feet in large part because the elevation angle is getting small.

These three examples should illustrate how difficult it will be to obtain altitude estimates accurate to preferably better than 100 feet. Simply averaging repeated sighting vectors (e.g., $\overrightarrow{v_1}$) is not an option, however, because the planes will always be moving at an appreciable velocity. Over observation intervals of 1 to even 120 seconds, a plane's heading, velocity, and altitude should be very slowly changing though. This means that it should be possible to greatly improve our estimate of the plane's position and velocity in spite of reasonable (ideally unbiased and nearly Gaussian) errors in the observation angles for each siting so long as estimates for the plane's motion are also used in the calculations. The mathematical theory behind such calculations is well known (e.g., Kalman filtering), and in fact plays a major role in the precision of modern GPS systems today. These details will be developed at length in future phases of the project.

2.3.2 Example Behavior with Straight Flight Path

It should come as no surprise with the appearance of trigonometric and square root functions in (8) and (9) that the azimuth and elevation angles will scribe out nonlinear paths over time thereby making the flight trajectory more interesting. Two example cases are shown below where the plane's velocity vector is assumed to be $\overrightarrow{v_p} = (100, 450, 0)$ ft/sec in the *x*-, *y*-, and *z*-directions respectively. In the first example, the initial position of the plane is assumed to be $\vec{P} = (25, 42, 24)$ kft whereas in the second example, it is assumed to be $\vec{P} = (35, 42, 35)$ kft. More investigation will be required in order to ascertain the best mathematical form for the plane's estimated flight path versus time.

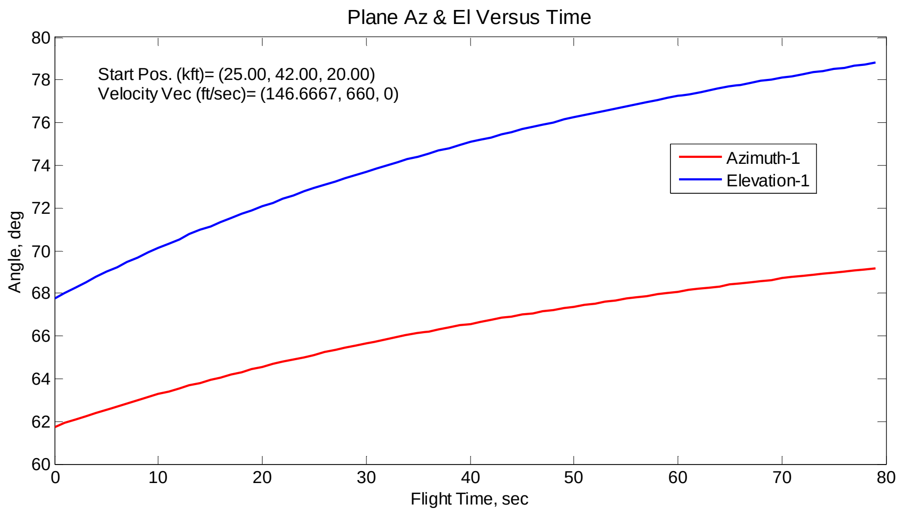

Figure 13 Example 1

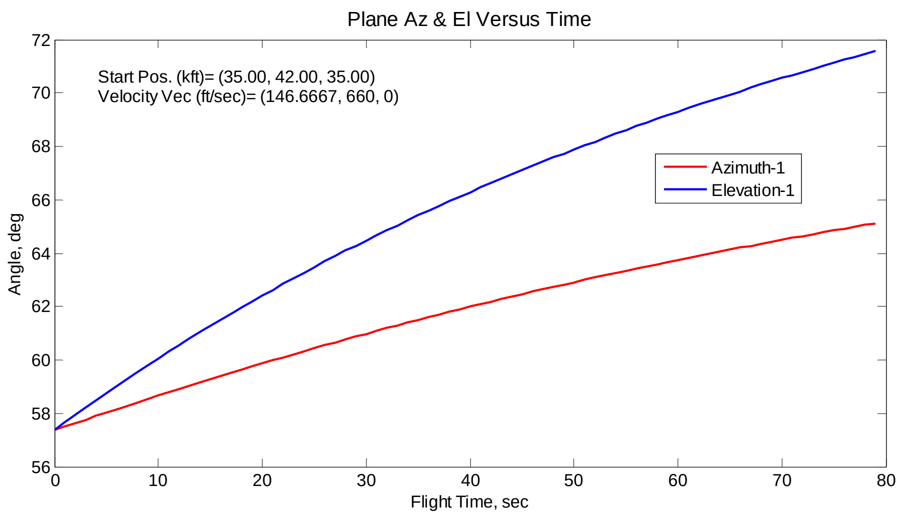

Figure 14 Example 2

3 Next Steps

The most demanding element of this project (at least for me) is telescope mount integrity at a reasonable cost. Even though the quality can be considerably worse than what would be required for deep-sky astrophotography, and imperfections like drive-train periodicity are likely less a concern because camera exposure times are much shorter, you have to get this part of the project correct or nothing else will matter that much. Consequently, the most important next-step is to run the equatorial mount plus telescope through the paces to make sure that angular repeatability in both right-ascension and declination (equatorial coordinates) are sufficiently good. Those results and more will be the subject of Part II.

